KSABC
The Korean Society for Applied Biological Chemistry

ARTICLE

Open Access

CircGAK inhibits cell growth, migration, invasion, and angiogenesis of hepatocellular carcinoma via miR-1323/HHIP axis

Hongchun Zhu, Shihong Lv, Baijing Yang, Zhuoxi Liu and Dan Zhang*

Abstract

Increasing evidence demonstrates that circular RNA (circRNA) plays a pivotal role in the development of disease, especially in Cancer. A previous circRNA microarray study showed that circGAK (hsa_circ_0005830) was remarkably down-regulated in hepatocellular carcinoma (HCC) tissues. However, the role of circGAK in HCC remains largely unclear. The candidate circRNAs were screened via integrating the Gene Expression Omnibus (GEO) database (GSE164803) analysis with the online program GEO2R. Quantitative real-time PCR (qRT-PCR) was employed to measure the expression of circGAK miR-1323, and hedgehog-interacting protein (HHIP) in HCC tissues and cells. The biological function of circ-GAK in HCC was examined using colony formation assay, 5-ethynyl-2'-deoxyuridine (EdU) assay, wound healing assay, transwell cell invasion assay, endothelial tubular formation assay, western blot assay, and xenograft mouse model. Bioinformatics analysis, RNA immunoprecipitation (RIP) assay, and dual-luciferase reporter assay were utilized to test the interaction between miR-1323, and circGAK or HHIP. The expression of circGAK was abnormally down-regulated in HCC tissues and was associated with the tumor-node-metastasis (TNM) stage. Overexpression of circGAK remarkably impeded HCC cell proliferation, migration, invasion, and endothelial tube formation in vitro, and tumor growth in vivo. Bioinformatics predicted that circGAK interacted with miR-1323, which targeted the HHIP mRNA 3'untranslated regions (UTR). Furthermore, upregulation of miR-1323 or shRNA-mediated HHIP suppression could recover circGAK-mediated malignant behaviors of HCC cells and tube formation of endothelial cells. Taken together, the circGAK/miR-1323/HHIP axis could suppress the progression of HCC and may provide potential new targets for the diagnosis and therapy of HCC.

Keywords: Hepatocellular carcinoma, circGAK, miR-1323, HHIP

Introduction

On a global scale, liver cancer is the sixth most commonly diagnosed cancer and the third most common cancer-related death rate in 2020 [1]. HCC is the main histological subtype of liver cancer, accounting for 90% of primary liver cancer [2]. Heredity, epigenetic changes, chronic hepatitis B, hepatitis C virus infection, aflatoxin exposure, smoking, obesity, and diabetes are the main risk factors for HCC [3]. Although comprehensive treatments are available, the prognosis of HCC is still unsatisfactory owing to recurrence and metastasis [4]. Therefore, it is urgent to seek new HCC diagnostic biomarkers and identify effective therapeutic targets to overcome these difficulties.

In general, the growth and survival of solid tumors depend on angiogenesis. Prior studies have pointed out that the increase of tumor cells must be accompanied by the formation of new capillaries [5]. Neovascularization not only provides nutrient supply to tumor cells through perfusion, and it is also an effective way of excreting tumor cell metabolites [5–7]. Numerous studies have

*Correspondence: zhcdzyx@126.com
Department of Gastroenterology, The Second Affiliated Hospital of Mudanjiang Medical College, NO. 15, East Xiaoyun Street, Aimin District, Mudanjiang 157000, China

Springer Open

Zhu *et al. Applied Biological Chemistry*   (2022) 65:48

Page 2 of 13

indicated that a variety of vascular growth factors, especially vascular endothelial growth factor A (VEGFA), produced by tumor cells could induce proliferation, migration, survival of tumor vascular endothelial cells, and promotion of angiogenesis in HCC [6, 8, 9]. Hence, inhibition of tumor angiogenesis may be used as a new treatment for HCC.

In recent years, as a new favorite in the field of non-coding RNA, circRNA has found new functions in various disorders [10]. circRNA is a circular structure produced by the back-splicing of pre-mRNA, which makes circRNA resistant to the degradation of RNA exonuclease and is more stable. Most circRNAs are formed by exon cyclization, and some circRNAs are nested structures formed by intron cyclization [11]. Moreover, circRNA contains a large number of microRNA (miRNA) response primitives (MREs), which can form an RNA-induced silencing complex with Ago protein and act as miRNA sponge to prevent miRNA from interacting with mRNA in the 3′UTR, thereby indirectly regulating the expression of downstream target genes of miRNA [12]. Recently, new evidence suggests that some circRNAs are involved in tumor malignant behaviors and angiogenesis [13]. For instance, circ-ERBIN was upregulated in colorectal cancer and could promote CRC growth, metastasis, and angiogenesis by sponging miR-125a-5p and miR-138-5p [14]. Besides, overexpression of hsa_circRNA_001587 could bind with miR-223 to elevate the expression of SLC4A4 and retard malignant behaviors and angiogenesis of pancreatic cancer [15]. Collectively, these observations underscore the importance of circRNA in tumor progression. However, the role and related molecular mechanisms of circRNA in HCC to a large extent are unknown.

In this study, we analyzed the circRNA profiling dataset GSE164803 to seek circRNAs of differential expression, and the results revealed that circGAK (circBase_ID: hsa_circ_0005830) was exceptionally decreased in HCC tissues compared to noncancerous tissues. Additionally, increased expression of circGAK could repress HCC cell proliferation, migration, invasion, and endothelial tube formation. Subsequently, we disclosed that circGAK may suppress the progression of HCC through the miR-1323/HHIP axis. CircGAK might serve as a novel favorable prognosis factor and therapeutic target in GC. The circGAK/miR-1323/HHIP axis would be expected to provide an opportunity to diagnose and treatment of HCC.

Materials and methods
Microarray datasets
GSE164803 dataset was downloaded from the GEO database and was analyzed with the GEO2R tool. GSE164803 included 6 HCC tissues and 6 normal tissues. The adj.P.Value < 0.05 was set as the threshold for screening the differentially expressed circRNAs.

Patient samples
HCC tumor tissues and adjacent noncancerous tissues (Normal) were collected from 45 HCC patients by surgery from the Second Affiliated Hospital of Mudanjiang Medical College. All participants received written informed consent. The isolated tissues were deposited at -8 ℃ until the next detection. This research was approved by the Medical Ethics Committee of the Second Affiliated Hospital of Mudanjiang Medical College.

Cell culture
The human HCC cells HCCLM6 (Liver Cancer Institute, Fudan University, Shanghai, China), human HCC cells MHCC97-H (Beyotime, Shanghai, China), and Human Embryonic Kidney Cells (293 T; Beyotime) were maintained in DMEM medium (10% FBS; Procell, Wuhan, China). Transformed Human Liver Epithelial-2 cells (THLE-2; ATCC, Manassas, VA, USA) was maintained in BEGM Bullet Kit (10% FBS; Lonza, Basel, Switzerland). Human Umbilical Vein Endothelial Cells (HUVEC; ATCC) were maintained in EGM-2 Endothelial Cell Growth Medium-2 Bullet Kit (10% FBS; Lonza). All cells were cultured at 37 ℃ with 5% CO_2.

qRT-PCR
Total RNA Extractor (Trizol; Songon, Shanghai, China) was employed to extract RNA of tissues and cells. The miRNA 1st Strand cDNA Synthesis Kit (by stem-loop; Vazyme, Nanjing, China) and AMV First Strand cDNA Synthesis Kit (For circRNA and mRNA; Songon) were performed to synthesize cDNA. The expression of circGAK, miR-324-3p, miR-1323, and HHIP mRNA was amplified using 2×SYBR Green PCR Mastermix (Solarbio, Beijing, China) and was measured by qRT-PCR ($2^{-\Delta\Delta CT}$ method). β-actin or U6 was for the reference gene. The primers were listed in Table 1.

Western blot assay
The protein of tissues and cells was extracted using Total Protein Extraction Kit (Strong; Solarbio) and was quantitated by BCA Protein Assay Kit (Solarbio). 30 μg protein was electrophoresed on 10% SDS-PAGE and was electrotransferred onto the membranes of PVDF (Solarbio). The membranes were blocked with 5% defatted dry milk and were incubated with primary antibodies against G1/S-specific cyclin-D1 (Cyclin D1; 1:200; ab16663; Abcam, Cambridge, UK), Matrix metalloproteinase-9 (MMP9; 1:5000; ab76003; Abcam), Vascular endothelial growth factor (VEGFA; 1:4000; ab52917; Abcam), HHIP (1:2000; PA5-115,355; Invitrogen, Carlsbad, CA, USA),

Zhu *et al. Applied Biological Chemistry*   (2022) 65:48

Page 3 of 13

Name		Primers for PCR (5′-3′)
circGAK(hsa_circ_0005830)	Forward	GTCCAGTTTTGTTCTGCAGCG
	Reverse	ACACAAATGCAAACCCTCCTTTA
HHIP	Forward	TCTCAAAGCCTGTTCCACTCA
	Reverse	GCCTCGGCAAGTGTAAAAGAA
miR-1323	Forward	TTCCGAGTCAAAACTGAGGGG
	Reverse	CTCAACTGGTGTCGTGGAGT
miR-324-3p	Forward	GTAATCCCACTGCCCCAGGT
	Reverse	AACTGGTGTCGTGGAGTCGG
18S rRNA	Forward	GGAGTATGGTTGCAAAGCTGA
	Reverse	ATCTGTCAATCCTGTCCGTGT
U6	Forward	CTTCGGCAGCACATATACT
	Reverse	AAAATATGGAACGCTTCACG
β-actin	Forward	CTTCGCGGGCGACGAT
	Reverse	CCACATAGGAATCCTTCTGACC

and β-actin (1:2000; K101527P; Solarbio) overnight at 4 ℃, respectively. Next, the membranes were added with a secondary antibody at 25 ℃ for 2 h. The protein signals were visualized by the EasyBlot ECL kit (Songon).

RNase R treatment
The RNA of HCCLM6 and MHCC97-H cells were processed with RNase R (Geneseed, Guangzhou, China) at 37 ℃ for 30 min. qRT-PCR and agarose gel electrophoresis was used to explore RNA expression of circGAK and β-actin.

Nuclear/cytoplasmic fractionation
PARIS™ Kit (Invitrogen) was employed to separate nuclear and cytoplasmic RNA of HCCLM6 and MHCC97-H cells. The expression levels of circGAK, 18S rRNA, and U6 were estimated by qRT-PCR.

Plasmid and oligonucleotides
Full-length circGAK and shRNA targeting HHIP were respectively cloned into lentiviral vector pLO5-ciR (pLO5-ciR-circGAK; Geneseed) and pLKO.1-puro (pLKO.1-puro-sh-HHIP, Biofeng, Shanghai, China). The psPAX2 and pMD2G plasmids were obtained from Biofeng. pmiR-RB-Report™ plasmids containing wild type and mutated circGAK or HHIP-3′ UTR sequence were constructed by RiboBio (Guangzhou, China). The miR-1323 mimic (miR-1323), and negative controls (miR-NC) were synthesized by RiboBio.

Transfection
pLO5-ciR-circGAK, psPAX2, and pMD2G plasmid were co-transfected into 293 T cells for 48 h. Lentivirus supernatant was collected and filtered by a 0.45 μm aperture filter and was added with 8 μg/mL polybrene. HCCLM6 and MHCC97-H cells were infected with lentivirus supernatant including pLO5-ciR-circGAK to generate the cell lines that stably overexpressed circGAK. pLKO.1-puro-sh-HHIP, pLKO.1-puro-sh-NC, miR-NC, and miR-1323 were transiently transfected into HCCLM6 and MHCC97-H cells by Lipofectamine 3000 (Invitrogen).

Colony formation assay
Transfected HCCLM6 and MHCC97-H cells (400/well) were seeded in 12-well plates for 2 weeks and then were fixed with 20% methanol (Solarbio) and stained with 0.25% crystal violet (Solarbio). Image-Pro Plus software was used to estimate the numbers of the colony.

EdU assay
Transfected HCCLM6 and MHCC97-H cells (4000/well) were inoculated in 96-well plates for 24 h. Cell DNA replication activity was measured by Cell-Light EdU Apollo567 In Vitro Kit (RiboBio).

Wound healing assay
Transfected HCCLM6 and MHCC97-H cells (50,000/well) were seeded in 24-well plates for 24 h and were scratched with a 10 μL pipette tip. Cells were washed with PBS and then was cultured with 1% FBS DMEM medium with 0.5 μg/mL Mitomycin C (Sigma-Aldrich, St. Louis, MO, USA). Image-Pro Plus software was employed to measure wound healing areas.

Transwell invasion assay
Transfected HCCLM6 and MHCC97-H cells (50,000/well) were suspended in 1% FBS DMEM medium and were seeded into the upper chamber of Corning Costar Transwell (Sigma-Aldrich) coated with matrigel (Solarbio). 15% FBS DMEM medium was added to the lower chambers. After 24 h, cells were fixed with 20% methanol (Solarbio). Non-invaded cells from the above side of the upper chamber were removed with a cotton swab and invaded cells were stained with 0.25% crystal violet (Solarbio). Cells of penetrated the lower surface were fixed and stained with 4% paraformaldehyde (Songon) and 0.2% crystal violet (Songon). Invaded cells were quantified by Image-Pro Plus software.

Endothelial tubular formation assay
Transfected HCCLM6 and MHCC97-H cells were cultured with serum-free DMEM medium for 24 h, and then the conditioned medium (CM) was collected and centrifuged to remove HCC cells. HUVEC cells (30,000/well) were cultured with aforesaid CM in 96-well plates coated

Zhu *et al. Applied Biological Chemistry*   (2022) 65:48

Page 4 of 13

with matrigel (Solarbio) for 12 h. The total tube length was quantified by Image-Pro Plus software.

RIP assay

RNA Immunoprecipitation Kit (Geneseed), Ago2 antibody (1:100; bs-12450R; Bioss), and rabbit IgG were employed to investigate the RNA of Ago2 binding. The enriched circGAK and miR-1323 were quantified by qRT-PCR.

Dual-luciferase reporter assay

miR-1323 or miR-NC was co-transfected with pmiR-RB-Report™ luciferase vectors containing wild type circGAK, mutated circGAK, wild type HHIP-3′ UTR, or mutated HHIP-3′ UTR into HCCLM6 and MHCC97-H cells for 48 h. The dual-Luciferase Reporter Gene Assay Kit (Songon) was used for detecting luciferase activity.

Animal experiments

MHCC97-H cells (2×10^6) that stable transfected circGAK or Vector were subcutaneously injected into the back of the left flank of BALB/c nude mice (Vital River, Beijing, China). So, the nude mice were divided into two groups, namely the Vector group (n = 5) and the circGAK group (n = 5). The volume was assessed with a caliper every 5 days and was calculated by the formula: Tumors volume $(mm^3) = (length \times width^2)/2$. After 30 days, the mice were euthanatized, and tumors were dissected and were used to examine weight, RNA expression (circGAK), protein expression (Cyclin D1, MMP9, VEGFA, HHIP, Ki-67, and CD31).

IHC assay

Mice tumor tissues fixed with 4% paraformaldehyde were embedded with paraffin and then were sliced. The sections were incubated with antibodies against Ki-67 (1:4000; 27,309–1-AP; Proteintech, Wuhan, China) and CD31 (1:2000; 11,265–1-AP; Proteintech), and the signal was detected using Rabbit specific HRP/DAB (ABC) IHC Detection Kit (Abcam).

Statistics

Data were shown as mean ± standard deviations (SD) and were statistically analyzed via GraphPad Prism 9. The comparison of two or more groups respectively used Student's *t*-test or one-way ANOVA with Tukey's post hoc test. The difference was deemed significant if $P < 0.05$.
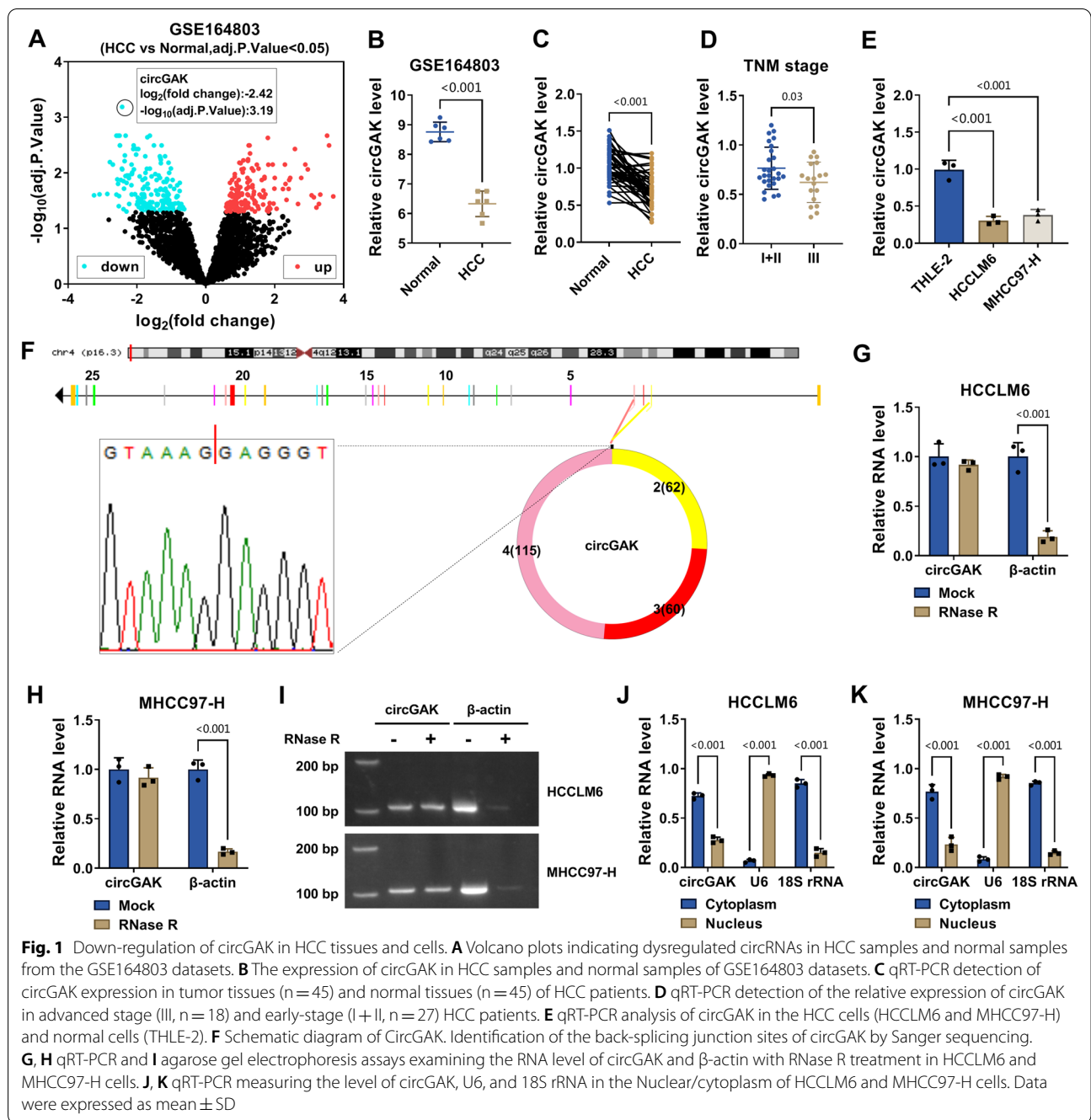
Results

CircGAK was found to be down-regulated in HCC tissues and cells

To identify the differentially expressed circRNAs in HCC, the microarray datasets GSE164803 were analyzed with the GEO2R tool. The differentially expressed circRNAs were visualized by volcano plots. Highlighted genes were significantly differentially expressed at a default adjusted p-value cutoff of 0.05. There were 153 upregulated circRNAs and 180 down-regulated circRNAs. Among these circRNAs, the expression of circGAK was reduced most obviously (Fig. 1A). In this study, circGAK was selected as a protagonist. Figure 1B showed that the expression of circGAK was down-regulated in 6 HCC tissues relative to 6 normal tissues in GSE164803 datasets. The expression of circGAK was significantly descended in tumor tissues versus the adjacent normal tissues of 45 HCC patients (Fig. 1C). Furthermore, in the advanced stage (III), the circGAK level was markedly less expressed than that in the early stage (I+II) of HCC patients (Fig. 1D). Similarly, the level of circGAK was prominently decreased in HCC cells (HCCLM6 and MHCC97-H) than that in normal cells (THLE-2) (Fig. 1E). Next, we found that circGAK was derived from the exons 2 to 4 of the GAK gene on chr4:905,460–907456[−], and the back-splice junction sites of circGAK were confirmed via Sanger sequencing (Fig. 1F). The qRT-PCR (Fig. 1G, H) and agarose gel electrophoresis (Fig. 1I) results displayed that circGAK was resistant to RNase R digestion, whereas linear β-actin mRNA was easily degraded. Notably, the qRT-PCR assay in nuclear/cytoplasmic fractions showed a predominant distribution of circGAK in the cytoplasm of HCCLM6 and MHCC97-H cells (Fig. 1J, K). Collectively, the above evidence concluded that the novel circGAK was down-regulated in HCC tissues and cells, implying it might be associated with the progression of HCC.

Overexpression of circGAK weakened HCC cells proliferation, migration, invasion, and HUVEC cells tube formation

To test whether circGAK was functional in HCC, we generated HCC cell lines that stably overexpressed circGAK for gene augment experiments. As shown in Fig. 2A, the expression of circGAK was significantly increased in HCCLM6 and MHCC97-H cells transfected with pLO5-ciR-circGAK (circGAK) in contrast to the pLO5-ciR (Vector). Next, the role of circGAK in HCC cell proliferation, migration, and invasion was analyzed with colony formation (Fig. 2B), EdU (Fig. 2C), wound healing (Fig. 2D), and transwell cell invasion assay (Fig. 2E). These results showed that the augment of circGAK suppressed proliferation, migration, and invasion in HCCLM6 and MHCC97-H cells. Previous studies had reported that tumor cells could promote angiogenesis in the tumor microenvironment [6]. Here we wondered if the augment of circGAK in HCC cells affected the endothelial tubular formation. To culture HUVECs, a conditioned medium (CM) was collected from HCCLM6 and MHCC97-H

Zhu *et al. Applied Biological Chemistry*   (2022) 65:48

Page 5 of 13

Fig. 1 Down-regulation of circGAK in HCC tissues and cells. **A** Volcano plots indicating dysregulated circRNAs in HCC samples and normal samples from the GSE164803 datasets. **B** The expression of circGAK in HCC samples and normal samples of GSE164803 datasets. **C** qRT-PCR detection of circGAK expression in tumor tissues (n = 45) and normal tissues (n = 45) of HCC patients. **D** qRT-PCR detection of the relative expression of circGAK in advanced stage (III, n = 18) and early-stage (I + II, n = 27) HCC patients. **E** qRT-PCR analysis of circGAK in the HCC cells (HCCLM6 and MHCC97-H) and normal cells (THLE-2). **F** Schematic diagram of CircGAK. Identification of the back-splicing junction sites of circGAK by Sanger sequencing. **G**, **H** qRT-PCR and **I** agarose gel electrophoresis assays examining the RNA level of circGAK and β-actin with RNase R treatment in HCCLM6 and MHCC97-H cells. **J**, **K** qRT-PCR measuring the level of circGAK, U6, and 18S rRNA in the Nuclear/cytoplasm of HCCLM6 and MHCC97-H cells. Data were expressed as mean ± SD
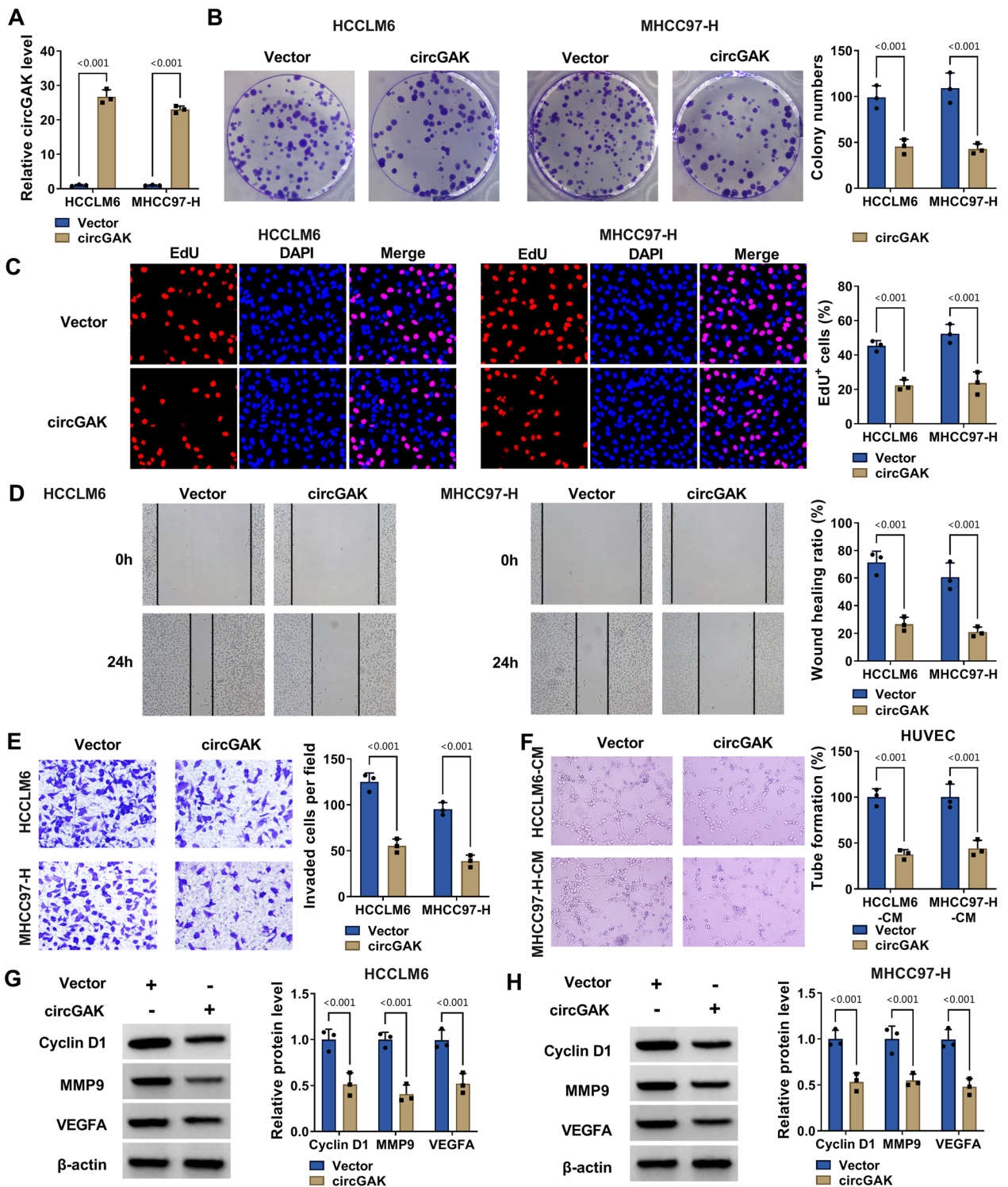
cells of overexpression circGAK. It was revealed in endothelial tubular formation assay that tube formation efficiency of HUVECs was dramatically reduced in the circGAK group with respect to the Vector group (Fig. 2F). Previous results have shown that Cyclin D1, MMP9, and VEGFA play an important role in promoting HCC cell proliferation, metastasis, and angiogenesis. Next, we detected the protein level of Cyclin D1, MMP9, and VEGFA. Western blot assay results presented that

increased circGAK constrained the expression of Cyclin D1, MMP9, and VEGFA (Fig. 2G, H).

CircGAK sponged miR-1323 in HCC cells

Given that circRNA may act as a sponge for miRNAs in the cytoplasm [16]. Firstly, the starBase database (https://starbase.sysu.edu.cn) [17] was applied to predict the potential miRNAs of circGAK binding. There were 7 miRNAs (miR-324-3p, miR-187-3p, miR-1913,

Zhu *et al. Applied Biological Chemistry*　　　(2022) 65:48

Page 6 of 13

Fig. 2 Function of circGAK in HCC cell proliferation, migration, and invasion as well as angiogenesis. **A** qRT-PCR detection of overexpression efficiency of circGAK. Cell proliferation activity as revealed by **B** colony formation assay and **C** EdU assay. **D** Cell migration and **E** cell invasion as revealed by wounding healing and transwell assays. **F** Tube formation of HUVECs after treated with supernatant derived from circGAK knockdown HCCLM6 and MHCC97-H cells. **G**, **H** WB analysis of the protein expression of Cyclin D1, MMP9, and VEGFA. Data were expressed as mean ± SD

Zhu *et al. Applied Biological Chemistry* (2022) 65:48

Page 7 of 13

miR-337-3p, miR-324-3p, miR-345-5p, and miR-1323) that had binding sites to circGAK. Then, we found that miR-324-3p and miR-1323 were upregulated in Liver Hepatocellular Carcinoma (LIHC) by the tool "Pan-Cancer" of the StarBase database (Fig. 3A). Further analysis of miR-324-3p and miR-1323 expression in five pairs of HCC specimens (Fig. 3B), and up-regulated miR-1323 was further validated by qRT-PCR in 45 pairs of HCC specimens (Fig. 3C). Compared with early-stage (I+II) patients, expression of miR-1323 was increased in advanced stage (III) of HCC patients (Fig. 3D). Furthermore, circGAK level was also upregulated in HCC cells (Fig. 3E). To assess whether circGAK acted as a sponge for miR-1323, we used the Ago2 RIP

assay. Compared with IgG, the Ago2 antibody enriched more circGAK and miR-1323, suggesting that circGAK might have interactions with miR-1323 in Ago2 protein (Fig. 3F, G). Additionally, the circGAK fragment with wild type (circGAK-wt) or mutant (circGAK-mut) complementary binding sites for miR-1323 was constructed and inserted into pmiR-RB-Report™ luciferase vectors (Fig. 3H). The expression of miR-1323 was remarkably increased in HCCLM6 and MHCC97-H cells transfected with miR-1323 mimic (miR-1323) than NC mimic (miR-NC) (Fig. 3I). Dual-luciferase reporter assay results exhibited that miR-1323 effectively reduced the luciferase activity of the circGAK-wt, but not in circGAK-mut (Fig. 3J, K).
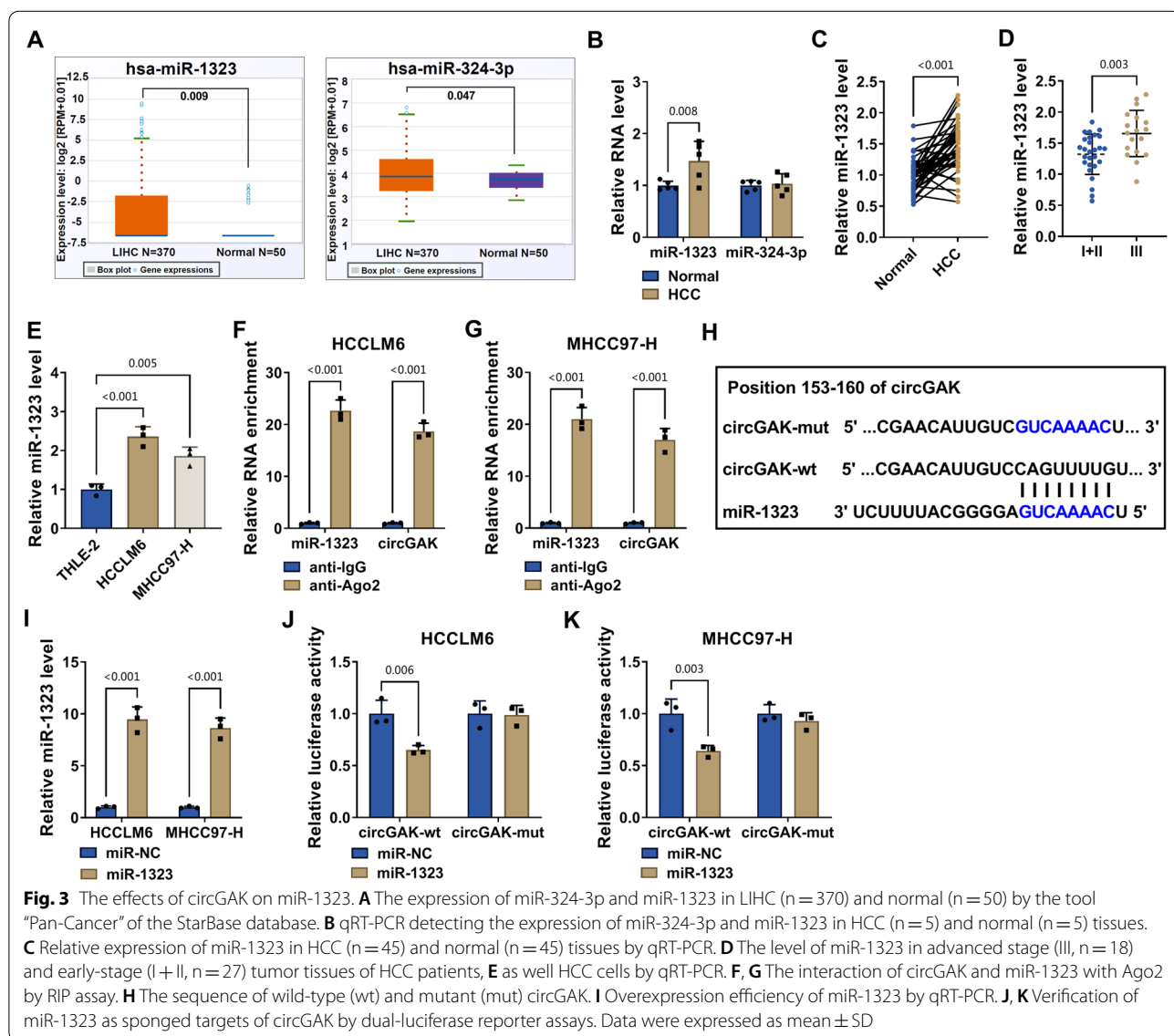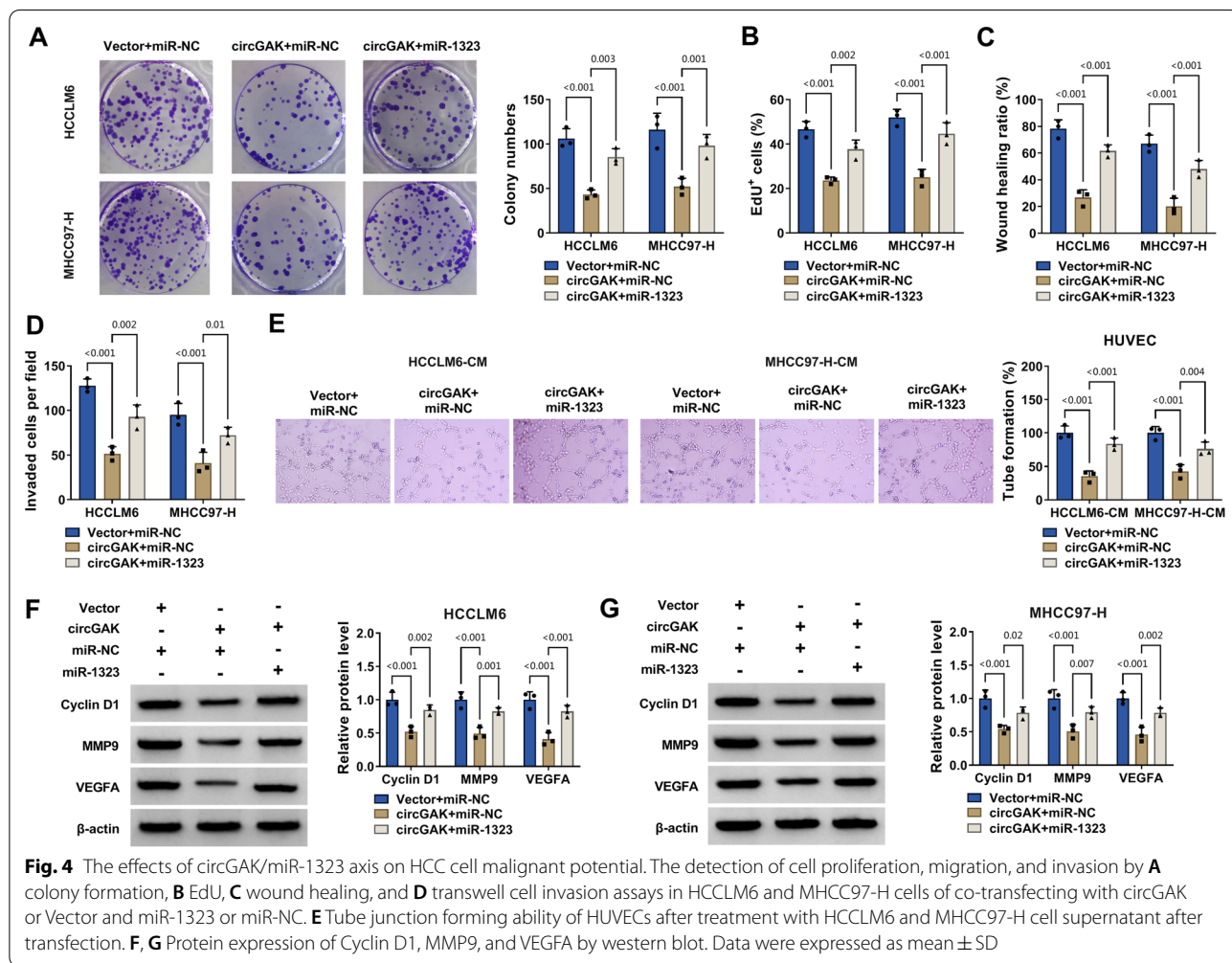

Fig. 3 The effects of circGAK on miR-1323. **A** The expression of miR-324-3p and miR-1323 in LIHC (n = 370) and normal (n = 50) by the tool "Pan-Cancer" of the StarBase database. **B** qRT-PCR detecting the expression of miR-324-3p and miR-1323 in HCC (n = 5) and normal (n = 5) tissues. **C** Relative expression of miR-1323 in HCC (n = 45) and normal (n = 45) tissues by qRT-PCR. **D** The level of miR-1323 in advanced stage (III, n = 18) and early-stage (I + II, n = 27) tumor tissues of HCC patients, **E** as well HCC cells by qRT-PCR. **F**, **G** The interaction of circGAK and miR-1323 with Ago2 by RIP assay. **H** The sequence of wild-type (wt) and mutant (mut) circGAK. **I** Overexpression efficiency of miR-1323 by qRT-PCR. **J**, **K** Verification of miR-1323 as sponged targets of circGAK by dual-luciferase reporter assays. Data were expressed as mean ± SD

Zhu *et al. Applied Biological Chemistry*   (2022) 65:48

Page 8 of 13

miR-1323 attenuated the inhibitory effect of circGAK on malignant behaviors of HCC
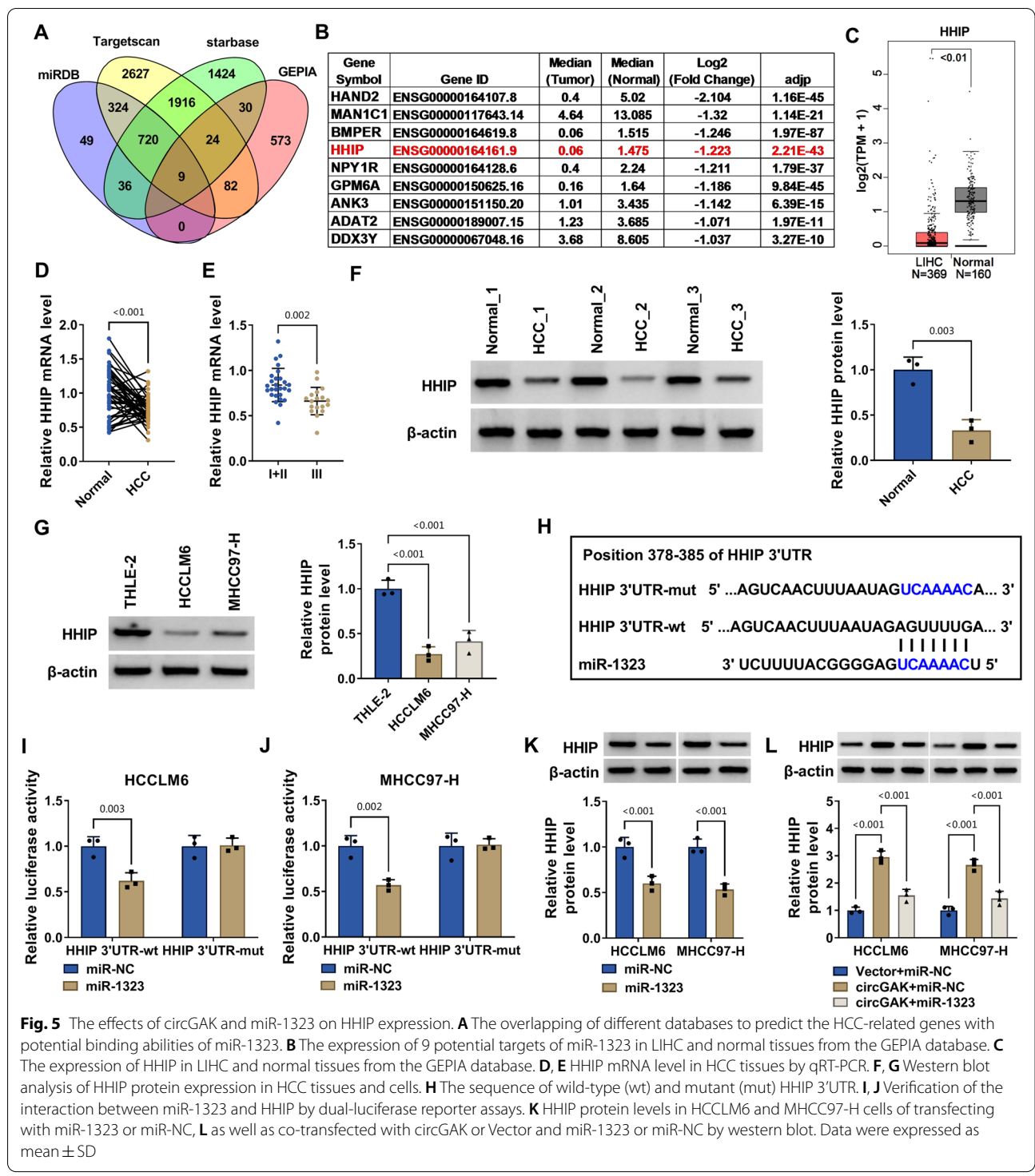
To further clarify the effect of miR-1323 on HCC cell phenotype, miR-1323 was transfected into HCCLM6 and MHCC97-H cells with upregulated circGAK. Results of EdU (Fig. 4A), colony formation assay (Fig. 4B), wound healing (Fig. 4C), and transwell cell invasion assay (Fig. 4D) uncovered that circGAK inhibited the proliferation, migration, and invasion of HCCLM6 and MHCC97-H cells, while miR-1323 could compromise these effects. Furthermore, the reduction of tube formation efficiency in HUVECs, which was induced by circGAK upregulation, was attenuated following overexpression of miR-1323 in HCCLM6 and MHCC97-H cells (Fig. 4E). Moreover, the expression of Cyclin D1, MMP9, and VEGFA was markedly down-regulated in the circGAK + miR-NC group, while after transfecting miR-1323, the expression levels of these proteins were upregulated (Fig. 4F, G).

miR-1323 directly interacted with HHIP

Firstly, bioinformatics tools Targetscan (http://www.targetscan.org/vert_72/) [18], miRDB (http://mirdb.org/) [19], and starbase were applied to predict the potential targets of miR-1323. The GEPIA database (http://gepia2.cancer-pku.cn/#index) [20] was used to selected the under-expressed gene ($\log_2FC < -1$ and q-value < 0.01) in LIHC (Fig. 5B). As shown in Figs. 5B, C, a total number of 9 potential targets of miR-1323 were under-expressed in LIHC. We further selected HHIP, which has been reported could act an anti-cancer role in HCC [21, 22], for a follow-up study. qRT-PCR results showed that HHIP mRNA level was down-regulated in HCC tumor tissues than normal tissues and reduced in tumor tissues of advanced stage (III) in comparison with early-stage (I+II) of HCC patients (Fig. 5D, E). The results of western blot demonstrated that HHIP protein level was markedly reduced in HCC tumor tissues (Fig. 5F) and cells (Fig. 5G) concerning normal tissues and normal cells. To confirm the direct interaction between miR-1323 and

Fig. 4 The effects of circGAK/miR-1323 axis on HCC cell malignant potential. The detection of cell proliferation, migration, and invasion by **A** colony formation, **B** EdU, **C** wound healing, and **D** transwell cell invasion assays in HCCLM6 and MHCC97-H cells of co-transfecting with circGAK or Vector and miR-1323 or miR-NC. **E** Tube junction forming ability of HUVECs after treatment with HCCLM6 and MHCC97-H cell supernatant after transfection. **F**, **G** Protein expression of Cyclin D1, MMP9, and VEGFA by western blot. Data were expressed as mean ± SD

Zhu *et al. Applied Biological Chemistry*   (2022) 65:48

Page 9 of 13

Fig. 5 The effects of circGAK and miR-1323 on HHIP expression. **A** The overlapping of different databases to predict the HCC-related genes with potential binding abilities of miR-1323. **B** The expression of 9 potential targets of miR-1323 in LIHC and normal tissues from the GEPIA database. **C** The expression of HHIP in LIHC and normal tissues from the GEPIA database. **D**, **E** HHIP mRNA level in HCC tissues by qRT-PCR. **F**, **G** Western blot analysis of HHIP protein expression in HCC tissues and cells. **H** The sequence of wild-type (wt) and mutant (mut) HHIP 3'UTR. **I**, **J** Verification of the interaction between miR-1323 and HHIP by dual-luciferase reporter assays. **K** HHIP protein levels in HCCLM6 and MHCC97-H cells of transfecting with miR-1323 or miR-NC, **L** as well as co-transfected with circGAK or Vector and miR-1323 or miR-NC by western blot. Data were expressed as mean ± SD

HHIP 3′UTR, the HHIP 3′UTR fragment with wild type (HHIP 3′UTR-wt) or mutant (HHIP 3′UTR-mut) complementary binding sites for miR-1323 was constructed and inserted into pmiR-RB-Report™ luciferase vectors (Fig. 5H). The dual-luciferase assay indicated that

miR-1323 could interact with the sites of HHIP 3′UTR (Fig. 5I, J). In addition, western blot results showed that the expression of HHIP protein was negatively regulated by miR-1323 (Fig. 5K). And the circGAK-induced increase in protein expression of HHIP was rescued by

Zhu *et al. Applied Biological Chemistry*   (2022) 65:48

Page 10 of 13

miR-1323 overexpression (Fig. 5L). Together, these data suggested that circGAK may target miR-1323 to regulate HHIP expression.

HHIP downregulation reversed the effects of circGAK overexpression in HCC cells

Given the previous results, we considered that HHIP might be involved in circGAK-restrained HCC progress. HCCLM6 and MHCC97-H cells of HHIP knockdown were generated by transducing them with pLKO.1-puro-sh-HHIP (sh-HHIP) (Fig. 6A). As for the cell function experiments in HCCLM6 and MHCC97-H cells, silencing of HHIP could rescue the inhibition of proliferation (Fig. 6B, C), migration (Fig. 6D), and invasion (Fig. 6E) caused by overexpression of circGAK. Additionally, the reduction of tube formation efficiency in HUVECs caused by circGAK upregulation was reverted by HHIP silencing (Fig. 6F). Western blot indicated that sh-HHIP

neutralized the decreased levels of Cyclin D1, MMP9, and VEGFA induced by circGAK (Fig. 6G, H). The above results allowed us to conclude that circGAK inhibited growth, migration, invasion, and angiogenesis of HCC via impeding HHIP expression.

CircGAK regulated HCC tumorigenesis in vivo

Finally, we performed a xenograft mouse model to evaluate the effects of the circGAK in HCC tumorigenesis in vivo. In comparison with the Vector group, the tumor volumes (Fig. 7A) and weights (Fig. 7B) were lessened in the circGAK group. circGAK expression was significantly elevated in the circGAK group (Fig. 7C). Moreover, western blot assay showed that HHIP expression was increased, the expression of Cyclin D1, MMP9, and VEGFA was reduced in tumor tissues of the circGAK group in contrast to the Vector group (Fig. 7D). We also detected tumor growth that was inhibited by limited
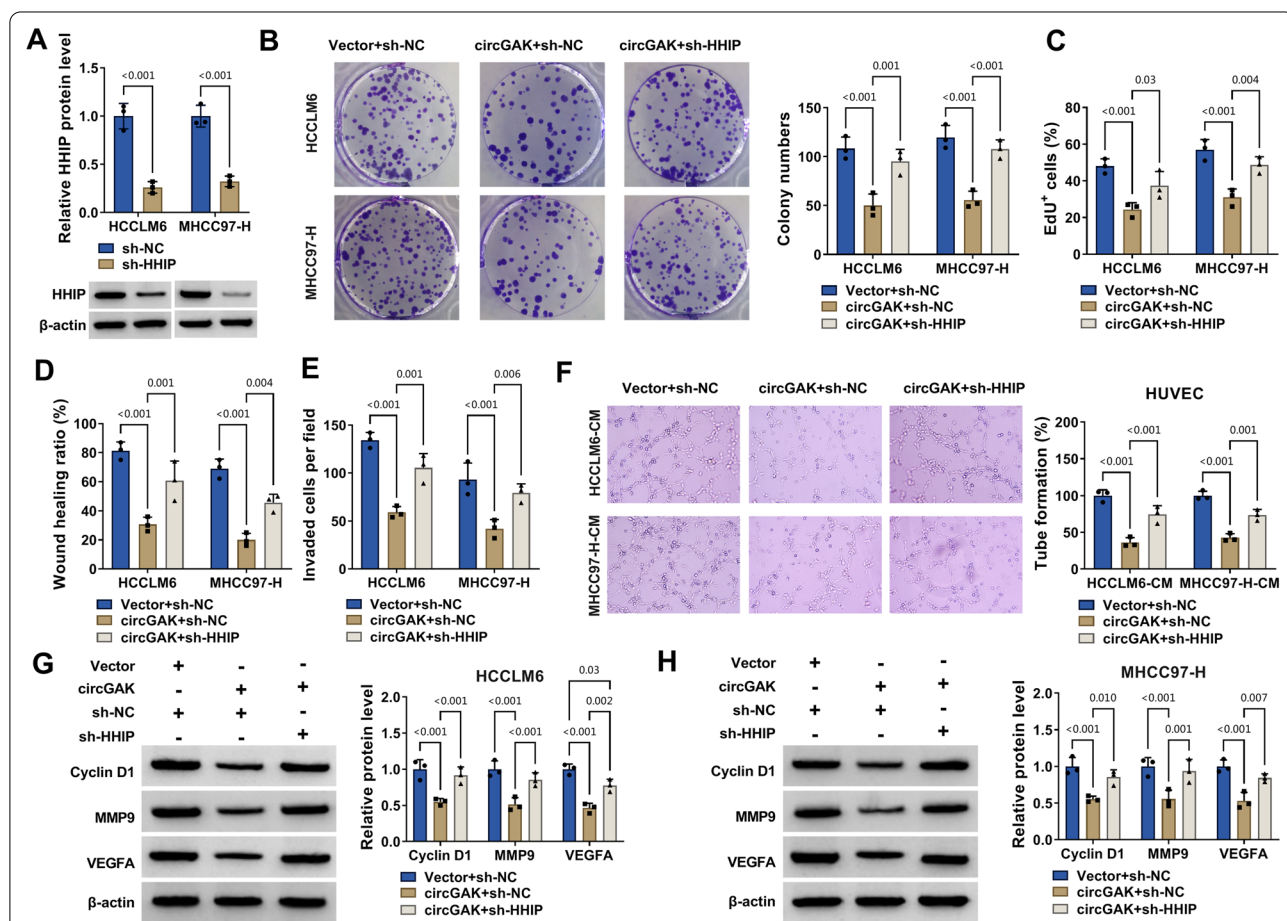
Fig. 6 The effects of circGAK/HHIP axis on HCC cell malignant potential. **A** Transfection efficacy of sh-HHIP in HCCLM6 and MHCC97-H cells via western blot. **B** Colony formation, **C** EdU, **D** wound healing, and **E** transwell cell invasion assay detecting cell proliferation, migration, and invasion in HCCLM6 and MHCC97-H cells of co-transfecting with circGAK or Vector and sh-NC or sh-HHIP. **F** Tube formation of HUVECs after treated with supernatant derived from HCCLM6 and MHCC97-H cells of co-transfecting with circGAK or Vector and sh-NC or sh-HHIP. **G**, **H** Western blot measuring Cyclin D1, MMP9, and VEGFA protein expression. Data were expressed as mean ± SD

Fig. 7 Inhibition of circGAK in HCC tumor growth in vivo. The effect of circGAK overexpression on **A** tumor volume and **B** tumor weight. **C** circGAK level in the circGAK group and Vector group by qRT-PCR. **D** The protein expression level of HHIP, Cyclin D1, MMP9, and VEGFA in the tumor tissues of the circGAK group and Vector group by western blot analysis. **E** The expression of Ki-67 and CD31 in tumor tissues by IHC. Data were expressed as mean ± SD

nutrient supply could be due to blocked tumor angiogenesis. IHC results disclosed that circGAK significantly reduced Ki-67 (a cell proliferation marker) and CD31 (a tumor angiogenesis marker) positive cells (Fig. 7E). These results confirmed that circGAK had robust anti-tumor growth and angiostatic effects in vivo.

expression.

Discussion

Although the level of research and development for the diagnosis and treatment of liver cancer has been unceasingly enhanced, its prognosis has not been significantly improved. The biggest obstacle affecting the treatment of HCC was its high metastasis rate and intense angiogenesis capacity [3]. Recent studies highlight the potential of circRNA as an important regulator of HCC. For instance, circASAP1 facilitated HCC cell growth and metastasis via the novel circASAP1-miR-326/miR-532-5p-MAPK1/ CSF-1 axis [23]. circ 0,004,018 could stabilize the expression level of TIMP2 by recruiting FUS in HCC cells, and the CM from HCC cells overexpressing circ_0004018 inhibited cell migration capacity and tube formation of HUVECs [8]. Highly expressed circMRPS35 may regulate the expression of STX3 by sponging miR-148a to promote proliferation, metastasis, and cisplatin resistance of HCC [24]. These findings suggested that circRNA may

be regarded as a potential RNA molecule for the treatment of HCC. In this study, by analyzing the expression of circRNAs in GSE164803 microarray datasets, we have uncovered that circGAK was distinctly down-regulated in HCC tissues. Reduced expression of circGAK followed by was proved in 45 pairs of HCC tissues and HCC cells. Moreover, low circGAK expression was associated with a higher TNM stage in HCC patients, suggesting that circGAK might serve a vital function in HCC prognosis and progression. Subsequently, we constructed gain of function experiments in HCCLM6 and MHCC97-H cells, which revealed that circGAK over-expression could inhibit HCC cell growth, migration, invasion, and retarded tube formation of HUVECs. Additionally, the augment of circGAK suppressed the tumor growth and angiogenesis in a xenograft mouse model.

It was previously found that the biological function of circRNA relied on its unique subcellular localization [16]. In our research, we found that circGAK was mainly located in the cytoplasm. It was well known that cytoplasmic circRNA could act as a miRNA decoy to influence mRNA translation or stability [16, 25]. Then, we demonstrated that miR-1323 was found up-regulated in HCC tissues and cells consistent with the prior studie s [26, 27]. Although there has been no research on the regulation of circGAK and miR-1323, miR-1323

Zhu *et al. Applied Biological Chemistry*   (2022) 65:48

Page 12 of 13

has been revealed to have pro-tumor effects in lung adenocarcinoma [28], esophageal squamous cell carcinoma [29], and HCC [26, 27]. For example, when compared with normal livers or adjacent non-malignant liver, miR-1323 was obviously up-regulated in HCC tumors [26]. Moreover, miR-1323 might be involved in GAS5-mediated tumor inhibition by targeting TP53INP1 [27]. Our study further presented that miR-1323 exerted a pro-tumor role by restoring circGAK-mediated inhibition on HCC cell growth, migration, invasion, and tube formation of HUVECs. Based on GEPIA, miRDB, TargetScan, and starbase, we found a total number of 9 potential targets (HAND2, MAN1C1, BMPER, HHIP, NPY1R, GPM6A, ANK3, ADAT2, and DDX3Y) of miR-1323 were under-expressed in LIHC. There were some results have suggested that MAN1C1 [30], HHIP [21, 22, 31, 32], and NPY1R [33] may play an inhibitory role in HCC. However, the expression and roles of HAND2, BMPER, GPM6A, ANK3, ADAT2, and DDX3Y have not been reported yet in HCC.

HHIP is a negative agent of the Hedgehog signaling pathway that is active, which can prevent the Hedgehog signaling system from being overactivated [34]. HHIP has been reported to inhibit tumor progression and metastasis of HCC [21, 22], gastric cancer [35], breast cancer [36], and non-small cell lung cancer [37]. It was worth noting that the Hedgehog signaling pathway could increase tumor cell growth and MMP expression to enhance cell metastasis, and promote angiogenesis by facilitating the expression of VEGF and angiopoietin in the tumor environment [32, 36, 38–41]. It was previously indicated that HHIP was conspicuously downregulated in HCC due to the hypermethylation of the HHIP gene promoter [32]. Moreover, HHIP could be acted as a tumor suppressor and could be regulated via the HHIP-AS1/HuR complex [21], CHB-PNALT exosomes containing miR-25-3p [31], and DIO3OS/miR-328 axis [22] in HCC. In this work, we also present that HHIP was reduced in HCC tissues and cells. In addition, HHIP may play an anti-tumor role through recuperating circGAK-mediated effects on HCC cell growth, migration, invasion, and tube formation of HUVECs. Nevertheless, whether the Hedgehog signaling pathway can be regulated by circGAK/miR-1323/HHIP axis needs further study.

This work has been constrained by the limitation of experimental conditions and has some shortcomings. To further study the mechanism of circGAK/miR-1323/HHIP axis on angiogenesis, it is needed to detect cell activity and migration of HUVECs by co-culture system in vitro and to measure new vessel density by the chick chorioallantoic membranes angiogenesis assay *in vivo*. Furthermore, the upstream regulatory mechanism of circGAK remains a significant challenge.

In summary, this study demonstrated that a new circGAK was down-regulated in HCC and correlated with the TNM stage. Specifically, circGAK constrained growth, migration, invasion, and angiogenesis of HCC by increasing the expression of HHIP via sponging miR-1323. Thus, the circGAK/miR-1323/HHIP axis may provide new insights into HCC therapeutic target.

References

1. Sung H, Ferlay J, Siegel RL, Laversanne M, Soerjomataram I, Jemal A et al (2021) Global cancer statistics 2020: GLOBOCAN estimates of incidence and mortality worldwide for 36 cancers in 185 countries. CA Cancer J Clin 71:209–249
2. Villanueva A (2019) Hepatocellular Carcinoma. New Engl J Med 380:1450–1462
3. Yang JD, Hainaut P, Gores GJ, Amadou A, Plymoth A, Roberts LR (2019) A global view of hepatocellular carcinoma: trends, risk, prevention and management. Nat Rev Gastroenterol Hepatol 16:589–604
4. Craig AJ, von Felden J, Garcia-Lezana T, Sarcognato S, Villanueva A (2020) Tumour evolution in hepatocellular carcinoma. Nat Rev Gastroenterol Hepatol 17:139–152
5. Folkman J (1971) Tumor angiogenesis: therapeutic implications. New Engl J Med 285:1182–1186
6. Morse MA, Sun W, Kim R, He AR, Abada PB, Mynderse M et al (2019) The Role of angiogenesis in hepatocellular carcinoma. Clin Cancer Res 25:912–920
7. Kuczynski EA, Vermeulen PB, Pezzella F, Kerbel RS, Reynolds AR (2019) Vessel co-option in cancer. Nat Rev Clin Oncol 16:469–493
8. Wu Y, Zhang M, Bi X, Hao L, Liu R, Zhang H (2021) ESR1 mediated circ_0004018 suppresses angiogenesis in hepatocellular carcinoma via recruiting FUS and stabilizing TIMP2 expression. Exp Cell Res 408:112804
9. Yu YX, Ge TW, Zhang P (2020) Circular RNA circGFRA1 promotes angiogenesis, cell proliferation and migration of hepatocellular carcinoma by combining with miR-149. Eur Rev Med Pharmacol Sci 24:11058–11064
10. Han B, Chao J, Yao H (2018) Circular RNA and its mechanisms in disease: from the bench to the clinic. Pharmacol Ther 187:31–44

11. Ebbesen KK, Kjems J, Hansen TB (2016) Circular RNAs: identification, biogenesis and function. Biochim Biophys Acta 1859:163–168
12. De N, Young L, Lau PW, Meisner NC, Morrissey DV, MacRae IJ (2013) Highly complementary target RNAs promote release of guide RNAs from human Argonaute2. Mol Cell 50:344–355
13. Shao Y, Lu B (2022) The emerging roles of circular RNAs in vessel co-option and vasculogenic mimicry: clinical insights for anti-angiogenic therapy in cancers. Cancer Metastasis Rev 41:173–191
14. Chen LY, Wang L, Ren YX, Pang Z, Liu Y, Sun XD et al (2020) The circular RNA circ-ERBIN promotes growth and metastasis of colorectal cancer by miR-125a-5p and miR-138-5p/4EBP-1 mediated cap-independent HIF-1α translation. Mol Cancer 19:164
15. Zhang X, Tan P, Zhuang Y, Du L (2020) hsa_circRNA_001587 upregulates SLC4A4 expression to inhibit migration, invasion, and angiogenesis of pancreatic cancer cells via binding to microRNA-223. Am J Physiol Gastrointest Liver Physiol 319:G703–G717
16. Hansen TB, Jensen TI, Clausen BH, Bramsen JB, Finsen B, Damgaard CK et al (2013) Natural RNA circles function as efficient microRNA sponges. Nature 495:384–388
17. Li JH, Liu S, Zhou H, Qu LH, Yang JH (2014) starBase v2.0: decoding miRNA-ceRNA, miRNA-ncRNA and protein-RNA interaction networks from large-scale CLIP-Seq data. Nucleic Acids Res 42:D92-97
18. Agarwal V, Bell GW, Nam J-W, Bartel DP (2015) Predicting effective microRNA target sites in mammalian mRNAs. eLife 4:e05005
19. Chen Y, Wang X (2020) miRDB: an online database for prediction of functional microRNA targets. Nucleic Acids Res 48:D127–D131
20. Tang Z, Li C, Kang B, Gao G, Li C, Zhang Z (2017) GEPIA: a web server for cancer and normal gene expression profiling and interactive analyses. Nucleic Acids Res 45:W98–W102
21. Bo C, Li X, He L, Zhang S, Li N, An Y (2019) A novel long noncoding RNA HHIP-AS1 suppresses hepatocellular carcinoma progression through stabilizing HHIP mRNA. Biochem Biophys Res Commun 520:333–340
22. Wang Z, Song L, Ye Y, Li W (2020) Long noncoding RNA DIO3OS hinders cell malignant behaviors of hepatocellular carcinoma cells through the microRNA-328/Hhip Axis. Cancer Manag Res 12:3903–3914
23. Hu ZQ, Zhou SL, Li J, Zhou ZJ, Wang PC, Xin HY et al (2020) Circular RNA sequencing identifies CircASAP1 as a key regulator in hepatocellular carcinoma metastasis. Hepatology (Baltimore, Md) 72:906–922
24. Li P, Song R, Yin F, Liu M, Liu H, Ma S et al (2022) circMRPS35 promotes malignant progression and cisplatin resistance in hepatocellular carcinoma. Mol Ther 30:431–447
25. Bartel DP (2004) MicroRNAs: genomics, biogenesis, mechanism, and function. Cell 116:281–297
26. Law PTY, Qin H, Ching AKK, Lai KP, Co NN, He M et al (2013) Deep sequencing of small RNA transcriptome reveals novel non-coding RNAs in hepatocellular carcinoma. J Hepatol 58:1165–1173
27. Zhang F, Yang C, Xing Z, Liu P, Zhang B, Ma X et al (2019) LncRNA GAS5-mediated miR-1323 promotes tumor progression by targeting TP53INP1 in hepatocellular carcinoma. OncoTargets Ther 12:4013–4023
28. Zhao H, Zheng C, Wang Y, Hou K, Yang X, Cheng Y et al (2020) miR-1323 promotes cell migration in lung adenocarcinoma by targeting Cbl-b and Is an early prognostic biomarker. Front Oncol 10:181
29. Chen Z, Yao N, Gu H, Song Y, Ye Z, Li L et al (2020) Circular RNA_LARP4 sponges miR-1323 and hampers progression of esophageal squamous cell carcinoma through modulating PTEN/PI3K/AKT pathway. Dig Dis Sci 65:2272–2283
30. Tu HC, Hsiao YC, Yang WY, Tsai SL, Lin HK, Liao CY et al (2017) Up-regulation of golgi α-mannosidase IA and down-regulation of golgi α-mannosidase IC activates unfolded protein response during hepatocarcinogenesis. Hepatol Commun 1:230–247
31. Ouyang Y, Tang Y, Fu L, Peng S, Wu W, Tan D et al (2020) Exosomes secreted by chronic hepatitis B patients with PNALT and liver inflammation grade ≥ A2 promoted the progression of liver cancer by transferring miR-25-3p to inhibit the co-expression of TCF21 and HHIP. Cell Prolif 53:e12833
32. Tada M, Kanai F, Tanaka Y, Tateishi K, Ohta M, Asaoka Y et al (2008) Down-regulation of hedgehog-interacting protein through genetic and epigenetic alterations in human hepatocellular carcinoma. Clin Cancer Res 14:3768–3776
33. Lv X, Zhao F, Huo X, Tang W, Hu B, Gong X et al (2016) Neuropeptide Y1 receptor inhibits cell growth through inactivating mitogen-activated protein kinase signal pathway in human hepatocellular carcinoma. Med Oncol 33:70
34. Sigafoos AN, Paradise BD, Fernandez-Zapico ME (2021) Hedgehog/GLI signaling pathway: transduction, regulation, and implications for disease. Cancers 13:3410
35. Song Y, Tu J, Cheng Y, Zhou F, Liu P, Zhou S et al (2020) HHIP overexpression suppresses human gastric cancer progression and metastasis by reducing Its CpG Island methylation. Front Oncol 10:1667
36. Qiu S, Chen G, Peng J, Liu J, Chen J, Wang J et al (2020) LncRNA EGOT decreases breast cancer cell viability and migration via inactivation of the hedgehog pathway. FEBS Open Bio 10:817–826
37. Zhao JG, Wang JF, Feng JF, Jin XY, Ye WL (2019) HHIP overexpression inhibits the proliferation, migration and invasion of non-small cell lung cancer. PLoS ONE 14:e0225755
38. Agrawal V, Kim DY, Kwon YG (2017) Hhip regulates tumor-stroma-mediated upregulation of tumor angiogenesis. Exp Mol Med 49:e289
39. Lee BNR, Son YS, Lee D, Choi YJ, Kwon SM, Chang HK et al (2017) Hedgehog-interacting protein (HIP) regulates apoptosis evasion and angiogenic function of late endothelial progenitor cells. Sci Rep 7:12449
40. Eichenmüller M, Gruner I, Hagl B, Häberle B, Müller-Höcker J, von Schweinitz D et al (2009) Blocking the hedgehog pathway inhibits hepatoblastoma growth. Hepatology (Baltimore, Md) 49:482–490
41. Tripathy A, Thakurela S, Sahu MK, Uthanasingh K, Behera M, Ajay AK et al (2018) The molecular connection of histopathological heterogeneity in hepatocellular carcinoma: a role of Wnt and hedgehog signaling pathways. PLoS ONE 13:e0208194

Publisher's Note